(12)

THE MIXED MODE CRACK PROBLEM IN A NONHOMOGENEOUS ELASTIC PLANE

by

Noboru Konda and F. Erdogan

Lehigh University, Bethlehem, PA

August 1992

FINAL PROJECT REPORT

OFFICE OF NAVAL RESEARCH CONTRACT NO. N0O014-89-3188

THE MIXED MODE CRACK PROBLEM IN A NONHOMOGENEOUS ELASTIC PLANE

by

Noboru Konda and F. Erdogan

Lehigh University, Bethlehem, PA

August 1992

FINAL PROJECT REPORT

OFFICE OF NAVAL RESEARCH CONTRACT NO. N0O014-89-3188

THE MIXED MODE CRACK PROBLEM IN A NONHOMOGENEOUS ELASTIC MEDIUM[1]

by

Noboru Konda[2] and F. Erdogan
Lehigh University, Bethlehem, PA 18015

ABSTRACT

In this paper a nonhomogeneous elastic medium containing a crack arbitrarily oriented with respect to the direction of property gradient is considered. The problem is solved under plane strain or generalized plane stress conditions. This is a highly simplified version of a class of physical problems that may arise in fracture mechanics studies of ceramic coatings, metal/ceramic composites and interfacial zones with continuously varying volume fractions or graded properties. The main results of the paper are the calculated modes I and II stress intensity fctors. Among the questions studied are the effects of the material nonhomogeneity constant, the crack orientation, the loading conditions, and the Poisson's ratio on the stress intensity factors. Briefly discussed are also the stress state near the crack tip and the crack opening displacement.

INTRODUCTION

Heterogeneous materials or various forms of composites have always been widely used in technological applications. These materials are generally designed in such a way that certain physical bulk properties of the medium are optimized. From a viewpoint of mechanical functioning, in practice most failure processes such as, for example, corrosion, wear, and fatigue appear to be surface related. Thus, to a certain extent many of these failures can be controlled by controlling the material properties near and at the surfaces. In some cases a relatively simple surface treatment would be sufficient as, for example, in surface hardening to prevent wear or in introducing residual compressive stresses to the surface to prevent fatigue

---

[1]This study was supported by NSF under the grant MSM-8613611, by the Office of Naval Research under the contract N00014-89-J-3188, and by Sumitomo Metal Industries, Ltd.

[2]Permanent address: Sumitomo Metal Industries, Ltd., Amagasaki, Japan.

crack initiation. In many other cases, however, a protective coating with a more resistant material may be needed. As some examples for such applications one may mention the thermal barrier ceramic coating of combustion chambers, engine blades and other components, coating of machine tools against wear, coatings used for protection against corrosion, and ion plating of parts by very low yield materials (such as gold or silver) to reduce friction.

In designing various coatings, in addition to their expected physical performance, their mechanical reliability as influenced by such failure related factors as cracking and debonding must also be taken into consideration. To a large extent the resistance of the material to such failures can be influenced through processing techniques (for example, by controlling the substrate temperature to influence the residual stresses, and by controlling the degree of mixing in plasma spray coating or in ion plating to influence the ductility of interfacial zones) (see Batakis and Vogan, 1985, and Houck, 1987). It is at this point that influencing material properties through tailoring the composition as well as controlling the processing techniques may be a practical option. It has been shown that certain strength related properties of ceramic coatings can be improved by layering the interfacial zone going from metal rich to ceramic rich compositions. For example, in joining tungsten to zirconia by introducing four intermediate layers that contain 80/20, 60/40, 40/60 and 20/80 percent W/ZrO_2, respectively, it was shown that the peak value of the residual stress becomes approximately one-sixth of that obtained from direct $W\text{-}ZrO_2$ bonding (Hirano, et al., 1988).

The next logical step is, of course, the processing of fully tailored materials and interfacial zones with predetermined continuously varying volume fractions. Advances in powder technology and surface chemistry in recent years have indeed made it possible to develop such nonhomogeneous materials (or functionally gradient materials) having metal and ceramic constituents (Hirano, et al., 1988; Hirano and Yamada, 1988). A different type of problem in which one would have to consider the material as being nonhomogeneous would be certain thermal stress problems. If the thermo-elastic constants are significantly dependent on the temperature and if the temperature variation in the medium is sufficiently high, then for realistic modelling and analysis the material has to be considered as being nonhomogeneous.

Fracture toughness and fatigue crack growth characterizations of the nonhomogeneous materials require the solution of certain standard crack problems. The mode I plane strain problem for an infinite nonhomogeneous medium (that is, the case of $\theta=0$ in Fig. 1) was considered by Delale and Erdogan (1983), who showed that the relative dependence of the stress intensity factors on the nonhomogeneity constant may be quite significant. Other crack problems involving various forms of material nonhomogeneity were considered by Kassir (1972), Dhaliwal and Singh (1978), Gerasaulis and Srivastav (1980), Erdogan (1985), and Delale and Erdogan (1988a, 1988b). In this paper, we consider the generral mixed mode plane

strain problem for an arbitrarily oriented crack in a nonhomogeneous medium. In previous studies it was shown that the effect of Poisson's ratio, ν, on the stres intensity factors is not very significant. Thus, in this study, too, ν is assumed to be constant.

FORMULATION OF THE CRACK PROBLEM

Consider the plane elasticity problem shown in Fig. 1 where the medium contains a finite crack on y=0 plane and has a shear modulus μ defined by

$$\mu(x_1) = \mu_o e^{\delta x_1} \quad , \quad \mu(x,y) = \mu_o e^{\beta x+\gamma y} \quad , \tag{1}$$

$$\beta = \frac{\delta}{\sqrt{1-\tan^2\theta}} \quad , \quad \gamma = \frac{\delta\tan\theta}{\sqrt{1-\tan^2\theta}} \quad , \tag{2}$$

μ_o and δ being material constants. By observing that $\kappa=3-\nu$ for plane strain and $\kappa = (3-\nu)/(1+\nu)$ for plane stress, and hence

$$\lambda(x,y) = \frac{3-\kappa}{\kappa-1}\,\mu_o e^{\beta x+\gamma y} \quad , \tag{3}$$

The Navier's equations for the elastic medium may be expressed as

$$(\kappa-1)\frac{\partial^2 u}{\partial x^2} + (\kappa-1)\frac{\partial^2 u}{\partial y^2} + 2\frac{\partial^2 v}{\partial x\partial y} + \beta(\kappa+1)\frac{\partial u}{\partial x} + \gamma(\kappa-1)\frac{\partial u}{\partial y} + \gamma(\kappa-1)\frac{\partial v}{\partial x}$$

$$- \beta(3-\kappa)\frac{\partial v}{\partial y} = 0 \, ,$$

$$(\kappa-1)\frac{\partial^2 v}{\partial x^2} + (\kappa+1)\frac{\partial^2 v}{\partial y^2} + 2\frac{\partial^2 u}{\partial x\partial y} + \gamma(3-\kappa)\frac{\partial u}{\partial x} + \beta(\kappa-1)\frac{\partial u}{\partial y} + \beta(\kappa-1)\frac{\partial v}{\partial x}$$

$$+ \gamma(\kappa+1)\frac{\partial v}{\partial y} = 0 \quad , \tag{4a.b}$$

where u and v are respectively the x and y ccomponents of the displacement vector. After separating the solution of the uncracked medium subjected to the prescribed external loads, the perturbation problem would have to be solved under the following boundary conditions and self-equilibrating crack surface tractions p_1 and p_2:

$$\sigma_{yy}(x,+0) = \sigma_{yy}(x,-0) \quad . \quad \sigma_{xy}(x,+0) = \sigma_{xy}(x,-0) \tag{5a.b}$$

$$v(x,+0)-v(x,-0) = 0 \; , \; |x|>a: \quad \sigma_{yy}(x,+0) = p_1(x) \; , \; |x|<a \; . \tag{6a.b}$$

$$u(x,+0)-u(x,-0) = 0, \; |x|>a: \quad \sigma_{xy}(x,+0) = p_2(x) \; , \; |x|<a \; . \tag{7a.b}$$

By expressing the solution of (4) as

$$u(x,y) = \frac{1}{2\pi} \int_{-\infty}^{\infty} U(y,\alpha)e^{-i\alpha x}d\alpha \quad ,$$

$$v(x,y) = \frac{i}{2\pi} \int_{-\infty}^{\infty} V(y,\alpha)e^{-i\alpha x}d\alpha \quad . \tag{8a.b}$$

we find

$$U(y,\alpha) = \sum_{j=1}^{4} m_j F_j(\alpha)e^{n_j y} \quad , \quad V(y,\alpha) = \sum_{j=1}^{4} F_j(\alpha)e^{n_j y} \quad , \tag{9a.b}$$

where $F_1,\ldots,F_4$ are unknown functions, $n_1,\ldots,n_4$ are the roots of

$$n^4 + 2\gamma n^3 + [-2\alpha(\alpha+i\beta) + \gamma^2 + \beta^2 \frac{\kappa-3}{\kappa+1}]n^2 + \alpha\gamma(-2\alpha-i\beta \frac{8}{\kappa+1})n$$

$$+ \alpha^2(\alpha^2+2i\alpha\beta-\beta^2+\gamma^2 \frac{3-\kappa}{\kappa+1}) = 0 \quad , \tag{10}$$

and $m_1,\ldots,m_4$ are given by

$$m_j = \frac{[i2\alpha-\beta(3-\kappa)]n_j+i(\kappa-1)\alpha\gamma}{(\kappa-1)n_j^2+(\kappa-1)\gamma n_j-(\kappa+1)\alpha(\alpha+i\beta)} \quad , \; j = 1,\ldots,4 \; . \tag{11}$$

It can be shown that the characteristic equation (10) may be expressed as follows:

$$[n^2+\gamma n-\alpha(\alpha+i\beta)]^2 + \frac{3-\kappa}{\kappa-1} (\alpha\gamma-i\beta n)^2 = 0 \quad . \tag{12}$$

From (12) it then follows that

$$n_1 = -\frac{\Delta_1}{2} - \frac{\sqrt{\Delta_1^2+4(\alpha^2+i\alpha\Delta_2)}}{2} \quad , \quad n_3 = -\frac{\Delta_1}{2} + \frac{\sqrt{\Delta_1^2+4(\alpha^2+i\alpha\Delta_2)}}{2} \; ,$$

$$n_2 = -\frac{\Delta_3}{2} - \frac{\sqrt{\Delta_3^2+4(\alpha^2+i\alpha\Delta_4)}}{2} \quad , \quad n_4 = -\frac{\Delta_3}{2} + \frac{\sqrt{\Delta_3^2+4\alpha^2+i\alpha\Delta_4)}}{2} . \tag{13a-d}$$

$$\Delta_1 = \sqrt{\frac{3-\kappa}{\kappa-1}}\,\beta-\gamma \quad , \quad \Delta_3 = -\sqrt{\frac{3-\kappa}{\kappa+1}}\,\beta+\gamma \quad .$$

$$\Delta_2 = \beta - \sqrt{\frac{3-\kappa}{\kappa-1}}\,\gamma \quad , \quad \Delta_4 = \beta + \sqrt{\frac{3-\kappa}{\kappa-1}}\,\gamma \quad . \tag{14a-d}$$

Since u and v must vanish for $x^2+y^2 \to \infty$, from (9) and (13) it follows that

$$F_3(\alpha) = F_4(\alpha) = 0 \quad , \quad y > 0 \quad . \tag{15a,b}$$

$$F_1(\alpha) = F_2(\alpha) = 0 \quad , \quad y < 0 \quad . \tag{16a,b}$$

By using the Hooke's Law, from (8), (9), (15) and (16) we obtain

$$\sigma_{xx}(x,y) = \frac{1}{2\pi}\int_{-\infty}^{\infty}\sum_{j=\ell}^{\ell+1}[-i\alpha m_j(2\mu+\lambda)+n_j\lambda]F_j\exp(n_jy)\exp(-i\alpha x)d\alpha \quad , \tag{17}$$

$$\sigma_{yy}(x,y) = \frac{1}{2\pi}\int_{-\infty}^{\infty}\sum_{j=\ell}^{\ell+1}[-i\alpha n_j\lambda+n_j(2\mu+\lambda)]F_j\exp(n_jy)\exp(-i\alpha x)d\alpha \quad , \tag{18}$$

$$\sigma_{xy}(x,y) = \frac{1}{2\pi}\int_{-\infty}^{\infty}\sum_{j=\ell}^{\ell+1}[n_jm_j-i\alpha]F_j\exp(n_jy)\exp(-i\alpha x)d\alpha \quad . \tag{19}$$

where $\ell=1$ for $y>0$ and $\ell=3$ for $y<0$. If we now substitute from (18) and (19) into the homogeneous conditions (5), we find

$$F_3 = R_1F_1 + R_2F_2 \quad , \quad F_4 = R_3F_1 + R_4F_2 \tag{20a,b}$$

where the known functions $R_1(\alpha).....R_4(\alpha)$ are given by

$$R_1(\alpha) = \{(m_4-m_1)[(1+\kappa)n_1n_4+(3-\kappa)\alpha^2]+i\alpha(n_4-n_1)[1+\kappa-(3-\kappa)m_1m_4]\}/R_0 \quad ,$$

$$R_2(\alpha) = \{(m_4-m_2)[(1+\kappa)n_2n_4+(3-\kappa)\alpha^2]+i\alpha(n_4-n_2)[1+\kappa-(3-\kappa)m_2m_4]\}/R_0 \quad .$$

$$R_3(\alpha) = -\{(m_3-m_1)[(1+\kappa)n_1n_3-(3-\kappa)\alpha^2]+i\alpha(n_3-n_1)[1+\kappa-(3-\kappa)m_1m_3]\}/R_0 ,$$

$$R_4(\alpha) = -\{(m_3-m_2)[(1+\kappa)n_2n_3+(3-\kappa)\alpha^2]-i\alpha(n_3-n_2)[1-\kappa-(3-\kappa)m_2m_3]\}/R_0 ,$$

$$R_0(\alpha) = (m_4-m_3)[(1-\kappa)n_3n_4+(3-\kappa)\alpha^2]+i\alpha(n_4-n_3)[1-\kappa-(3-\kappa)m_3m_4] . \qquad (21a-c)$$

The two remaining unknown functions F_1 and F_2 are determined from the mixed boundary cconditions (6) and (7).

THE INTEGRAL EQUATIONS

To reduce the problem to a system of integral equations we introduce the following new unknown functions:

$$g_1(x) = \frac{\partial}{\partial x}[u(x,-0)-u(x,0)] , \quad |x|<a$$

$$g_2(x) = \frac{\partial}{\partial x}[v(x,-0)-v(x,0)] , \quad |x|<a . \qquad (22a,b)$$

By substituting for u and v from the results found in the previous section and inverting the Fourier integrals, from (22) it may be shown that

$$\int_{-\infty}^{\infty} g_1(t)e^{i\alpha t}dt = -i\alpha(1-\kappa)[(f_{11}-i\alpha f_{41})F_1 + (f_{12}-i\alpha f_{42})F_2]/(4R_0) ,$$

$$\int_{-\infty}^{\infty} g_2(t)e^{i\alpha t}dt = -i\alpha\{[-(1-\kappa)f_{21}+i\alpha(3-\kappa)f_{31}]F_1 + [-(1+\kappa)f_{22}$$

$$+ i\alpha(3-\kappa)f_{32}]F_2\}/(4R_0) . \qquad (23a,b)$$

where

$$f_{1j} = n_3m_4m_j(n_4-n_j)+n_4m_3m_j(n_j-n_3)+n_jm_3m_4(n_3-n_4) ,$$

$$f_{2j} = m_4m_j(n_4-n_j)+m_3m_j(n_j-n_3)+m_3m_4(n_3-n_4) ,$$

$$f_{3j} = n_3m_3(n_4-n_j)+n_4m_4(n_j-n_3)+n_jm_j(n_3-n_4) ,$$

$$f_{4j} = m_3(n_4-n_j)+m_4(n_j-n_3)+m_j(n_3-n_4) , \quad j=1,2. \qquad (24a-d)$$

Equations (23) and (24) give the unknown functions F_1 and F_2 in terms of g_1 and g_2. On the other hand, by substituting from (18) and (19) into (6b) and (7b) we find

$$\lim_{y\to+0} \frac{1}{2\pi}\int_{-\infty}^{\infty} \sum_{j=1}^{2} [-i\alpha m_j\lambda+n_j(2\mu+\lambda)]F_j(\alpha)e^{n_jy-i\alpha x}d\alpha = p_1(x) \ , \ |x|<a \ ,$$

$$\lim_{y\to+0} \frac{1}{2\pi}\int_{-\infty}^{\infty} \sum_{j=1}^{2} \mu(n_jm_j-i\alpha)F_j(\alpha)e^{n_jy-i\alpha y}d\alpha = p_2(x) \ , \ |x|<a \ . \qquad (25a,b)$$

Now, solving (23) for F_1 and F_2, substituting into (25), and from (22), (6a) and (7a) observing that $g_j(t)=0$ for $|t|>a$, we obtain the following integral equations:

$$\lim_{y\to+0} \int_{-a}^{a} \sum_{j=1}^{2} h_{kj}(x,y,t)g_j(t)dt = \frac{\pi(\kappa+1)}{2\mu_0} e^{-\beta x}p_k(x) \ , \ |x|<a \ , \ k=1,2 \ , \qquad (26)$$

where

$$h_{kj}(x,y,t) = \int_{-\infty}^{\infty} K_{kj}(y,\alpha)e^{i\alpha(t-x)}d\alpha \ , \ k=1,2; \ j=1,2 \ , \qquad (27)$$

and the known functions K_{kj} are given in the Appendix. Since the conditions $g_j(t)=0$ rather than (6a) and (6b) are used for $|t|>a$ in deriving (26), the integral equations must be solved under the following single-valuedness conditions:

$$\int_{-a}^{a} g_j(t)dt = 0 \ , \ j=1,2 \ . \qquad (28)$$

In order to determine the possible singular behavior of (26), the behavior of the kernels h_{kj}, (k,j=1,2) at x=t and y=0 needs to be examined. For this, it is sufficient to determine and separate those leading terms in the asymptotic expansion of K_{kj} as $|\alpha|\to\infty$ that would lead to unbounded integrals. From the expressions of K_{kj} given in the Appendix it can be shown that in the asymptotic expansions for $\alpha\to\infty$ the only terms that would give unbounded integrals are

$$K_{12}^{\infty}(y,\alpha) = K_{21}^{\infty}(y,\alpha) = \frac{1}{2i}\frac{|\alpha|}{\alpha}e^{-|\alpha|y} \ . \qquad (29)$$

Substituted into (27), these terms give Cauchy type kernels. The next lower order terms are of the form $1/|\alpha|$ and give at most logarithmic kernels, $\log|t-x|$ which are square integrable and may be treated as Fredholm kernels. By adding and subtracting the asymptotic values given

by (29) to and from K_{kj} in (27), and by evaluating the integrals involving the leading terms, (26) may be modified as follows:

$$\int_{-a}^{a}\left[\frac{g_2(t)}{t-x}+k_{11}(x,t)g_1(t)+k_{12}(x,t)g_2(t)\right]dt=\frac{\pi(1+\kappa)}{2\mu(x,0)}\,p_1(x)\ ,\ |x|<a\ .$$

$$\int_{-a}^{a}\left[\frac{g_1(t)}{t-x}+k_{21}(x,t)g_1(t)+k_{22}(x,t)g_2(t)\right]dt=\frac{\pi(1+\kappa)}{2\mu(x,0)}\,p_2(x)\ ,\ |x|<a\ . \qquad (30a,b)$$

where

$$k_{11}(x,t)=h_{11}(x,0,t)\ ,\ k_{22}(x,t)=h_{22}(x,0,t)\ .$$

$$k_{12}(x,t)=\int_{-\infty}^{\infty}\left[K_{12}(0,\alpha)-K_{12}^{\infty}(0,\alpha)\right]e^{i\alpha(t-x)}d\alpha\ .$$

$$k_{21}(x,t)=\int_{-\infty}^{\infty}\left[K_{21}(0,\alpha)-K_{21}^{\infty}(0,\alpha)\right]e^{i\alpha(t-x)}d\alpha\ . \qquad (31a\text{-}d)$$

SOLUTION AND THE STRESS INTENSITY FACTORS

To solve the system of integral equations (30) we first define the following normalized quantities:

$$s=t/a,\ r=x/a,\ g_i(t)=f_i(s),\ k_{ij}(x,t)=L_{ij}(r,s),\ p_i(x)=p_i(ar),\ (i,j=1,2). \qquad (32)$$

Then, for example, (30a) may be expressed as

$$\frac{1}{\pi}\int_{-1}^{1}\left[\frac{f_2(s)}{s-r}+\sum_{j=1}^{2}L_{1j}(r,s)f_j(s)\right]ds=\frac{1+\kappa}{2\mu(ar,0)}\,p_1(ar),\ |r|<1\ . \qquad (33a)$$

Noting that the fundamental solution of (33a) is $(1-s^2)^{-1/2}$, the unknown functions f_1 and f_2 may now be expressed as

$$f_1(s)=\sum_{n=0}^{\infty}\frac{A_nT_n(s)}{\sqrt{1-s^2}}\ ,\ f_2(s)=\sum_{n=0}^{\infty}\frac{B_nT_n(s)}{\sqrt{1-s^2}}\ , \qquad (34a,b)$$

where T_n is the Chebyshev polynomial of the first kind. From (28), (34) and the orthogonality conditions of $T_n(s)$ it may be seen that

$$A_o=0\ ,\ B_o=0\ . \qquad (35)$$

Thus, by substituting from (34) into (33) and by using the properties

$$\frac{1}{\pi}\int_{-1}^{1}\frac{T_n(s)ds}{(s-r)\sqrt{1-s^2}}=\begin{cases} U_{n-1}(r)\ , & |r|<1 \\ -\dfrac{(r-\frac{r}{|r|}\sqrt{r^2-1})^n}{\frac{|r|}{r}\sqrt{r^2-1}}\ , & |r|>1 \end{cases} \tag{36}$$

we find

$$\sum_{n=1}^{\infty}B_nU_{n-1}(r)-\frac{1}{\pi}\sum_{n=1}^{\infty}\int_{-1}^{1}[A_nL_{11}(r,s)+B_nL_{12}(r,s)]\frac{T_n(s)}{\sqrt{1-s^2}}\,ds$$

$$=\frac{(1-\kappa)p_1(ar)}{2\mu(ar,0)}\ ,\quad |r|<1\ ,$$

$$\sum_{n=1}^{\infty}A_nU_{n-1}(r)-\frac{1}{\pi}\sum_{n=1}^{\infty}\int_{-1}^{1}[A_nL_{21}(r,s)+B_nL_{22}(r,s)]\frac{T_n(s)}{\sqrt{1-s^2}}\,ds$$

$$=\frac{(1-\kappa)p_2(ar)}{2\mu(ar,0)}\ ,\quad |r|<1\ , \tag{37a,b}$$

where $U_n(r)$ is the Chebyshev polynomial of the second kind. Note that the integrals in (37) are the Gaussian type and the solution may be obtained by truncating the series and using an appropriate collocation in r.

The stress intensity factors at the crack tips a and -a are defined by

$$k_1(a)=\lim_{x\to a}\sqrt{2(x-a)}\,\sigma_{yy}(x,0)\ ,\quad k_2(a)=\lim_{x\to a}\sqrt{2(x-a)}\,\sigma_{xy}(x,0)\ ,$$

$$k_1(-a)=\lim_{x\to -a}\sqrt{2(-x-a)}\,\sigma_{yy}(x,0)\ ,\quad k_2(-a)=\lim_{x\to -a}\sqrt{2(-x-a)}\,\sigma_{xy}(x,0)\ . \tag{38a-d}$$

To evaluate k_1 and k_2 we observe that equations (25), or (30) provide the expressions for $\sigma_{yy}(x,0)$ and $\sigma_{xy}(x,0)$ that are valid for $|x|>a$ as well as $|x|<a$. Thus, by using (36), and replacing $p_1(x)$ by $\sigma_{yy}(x,0)$ (for $|x|>a$), from (33) it may easily be shown that

$$k_1(a) = \lim_{x\to a} \sqrt{2(x-a)}\ \sigma_{yy}(x,0) = \lim_{r\to 1} \sqrt{a}\ \sqrt{2(r-1)}\ \sigma_{yy}(ar,0)$$

$$= \lim_{r\to 1} \sqrt{a}\ \sqrt{2(r-1)}\ \frac{2\mu(ar,0)}{1+\kappa}\left[\sum_{n=1}^{\infty} B_n\left(-\frac{(r-\frac{|r|}{r}\sqrt{r^2-1})^n}{\frac{|r|}{r}\sqrt{r^2-1}}\right) + F_1(r)\right],\ r>a \qquad (39)$$

where $F_1(r)$ represents all other bounded terms. Taking the limit in (39) we find

$$k_1(a) = -\sqrt{a}\ \frac{2\mu(a,0)}{1-\kappa}\sum_{n=1}^{\infty} B_n\ . \qquad (40)$$

Similarly

$$k_2(a) = -\sqrt{a}\ \frac{2\mu(a,0)}{1-\kappa}\sum_{n=1}^{\infty} A_n\ .$$

$$k_1(-a) = \sqrt{a}\ \frac{2\mu(-a,0)}{1+\kappa}\sum_{n=1}^{\infty} (-1)^n B_n\ .$$

$$k_2(-a) = \sqrt{a}\ \frac{2\mu(-a,0)}{1-\kappa}\sum_{n=1}^{\infty} (-1)^n A_n\ . \qquad (41a\text{-}c)$$

RESULTS

The main results of this study are the stress intensity factors that are obtained from (40) and (41) after solving equations (37), and are given in Tables 1-7. Referring to Fig. 1 we observe that the half crack length a is the only length parameter in the problem which may be eliminated by suitably normalizing all relevant quantities (see, for example, Eq. 32). The exponent δ in $\mu(x_1)=\mu_0\exp(\delta x_1)$ is the measure of material nonhomogeneity and appears as the nondimensional constant $a\delta$ in the results given. The angle θ defines the orientation of the crack with respect to the direction x_1 of the material property gradient. As physically expected, for $\theta=0$ the integral equations uncouple and the crack problems corresponding to modes I and II loading conditions can be solved separately. For $\theta\neq 0$ the integral equations are always coupled regardless of the loading conditions. Tables show the stress intensity factors k_1 and k_2 in normalized form. The basic definition of k_1 and k_2 are given by (38). The normalized stress intensity factors are defined by

$$k_1(\mp a) = k_1(\mp a)/(P\sqrt{a}) \qquad (42)$$

where P represents, in each case, the amplitude of the crack surface traction. Referring to (6b) and (7b), the following tractions were used in the examples given by the Tables:

$$p_2(x) = 0 \ , \ p_1(x) = (-\sigma_0, -\sigma_1 x/a \ , -\sigma_2 x^2/a^2 \ , -\sigma_3 x^3/a^3) \ . \tag{43}$$

$$p_1(x) = 0 \ , \ p_2(x) = (-\tau_0 \ , -\tau_1 x/a \ , -\tau_2 x^2/a^2 \ , -\tau_3 x^3/a^3) \ . \tag{44}$$

For crack surface tractions that are reasonably smooth functions of x, the stress intensity factors may be approximated by a suitable superposition of the results given by (43) and (44). It should be pointed out that in nonhomogeneous materials the external loading conditions in many cases may be modelled by prescribing displacements rather than tractions. The two practical cases that may be considered are the "uniform strain" and "bending" applied to the medium away from the crack region. It will be assumed that the displacements are prescribed in the planes parallel to the direction of the property gradient, x_1 in such a way that

$$\epsilon_{y_1 y_1}(x_1 = \pm\infty) = \epsilon_0 \ ,$$

$$\epsilon_{y_1 y_1}(x_1 = \pm\infty) = \epsilon_1 x_1 \ . \tag{45a,b}$$

By observing that $\mu = \mu_0 \exp(\delta x_1)$ and $x_1 = x\cos\theta + y\sin\theta$, in the perturbation problem the crack surface tractions corresponding to (45) may be expressed as

$$\sigma_{yy}(x,0) = -\frac{8\mu_0}{1+\kappa} \epsilon_0 e^{\delta x\cos\theta} \cos^2\theta \ ,$$

$$\sigma_{xy}(x,0) = \frac{8\mu_0}{1+\kappa} \epsilon_0 e^{\delta x\cos\theta} \sin\theta\cos\theta \ ; \tag{46a,b}$$

$$\sigma_{yy}(x,0) = -\frac{8\mu_0}{1+\kappa} \epsilon_1 x e^{\delta x\cos\theta} \cos^3\theta \ ,$$

$$\sigma_{xy}(x,0) = \frac{8\mu_0}{1+\kappa} \epsilon_1 x e^{\delta x\cos\theta} \sin\theta\cos^2\theta \ . \tag{47a,b}$$

where, depending on the constraint of the medium in z direction,

$$\frac{8\mu_0}{1+\kappa} = \begin{cases} E_0 \ , \text{ for plane stress.} \\ E_0/(1-\nu^2) \ , \text{ for plane strain .} \end{cases} \tag{48}$$

If the solid is uniformly stressed in x_1 direction (by prescribing u_1 or

$\sigma_{y_1y_1}(\mp\infty,y_1)=\sigma_o$), the corresponding crack surface tractions may be shown to be

$$\sigma_{yy}(x,0) = -\sigma_o\sin^2\theta \ , \ \sigma_{xy}(x,0) = -\sigma_o\sin\theta\cos\theta \ , \tag{49}$$

which, for a given crack orientation θ, are constant. Thus, the solution for the loading conditions (49) may be obtained by a proper superposition of the results found by using (43) and (44).

Table 1 shows the effect of $a\delta$ on the stress intensity factors for the two limiting crack orientations, $\theta=0$ and $\theta=\pi/2$ under a uniform crack surface pressure σ_o. For $\theta=0$ the crack results obtained are essentially the same as that found by Delale and Erdogan (1983). For $\theta=\pi/2$, $x=0$ is a plane of symmetry, the crack problem is one of mixed mode, and the mode II component becomes quite significant for larger values of $a\delta$. For the uniformly pressurized crack more detailed results are shown in Table 2 where the angle θ is varied between 0 and $\pi/2$. The results need to be examined rather carefully if one is interested in the fracture initiation at the crack tips. For example, one surprising result shown by Table 2 is that the maximum values of k_1 and k_2 do not generally correspond to the limiting crack orientations $\theta=0$ and $\theta=\pi/2$. This may be seen somewhat more clearly from Fig. 2 which shows the variation of the stress intensity factors with the angle θ for $a\delta=1$. Also, the values of θ corresponding to maximum stress intensity factors seem to depend on $a\delta$.

For a quick assessment of a possible crack growth initiation, it is generally sufficient to examine the amplitude and the direction of the maximum cleavage stress $\sigma_{\phi\phi}$ at the crack tips (see Erdogan and Sih, 1963). Given the stress intensity factors k_1 and k_2, the "cleavage" stress σ_{oo} in the small neighborhood of the crack tip may be expressed as

$$\sigma_{oo}(r,o) = \frac{1}{\sqrt{2r}}\left[k_1\cos^2\frac{o}{2} - \frac{3}{2}k_2\sin o\right]\cos\frac{o}{2} \ , \tag{50}$$

where (r,o) are the polar coordinates at the crack tip and ϕ is measured from the x axis. Generally the hypothesis is that the crack initiation would be radial in a direction ϕ^* perpendicular to the local maximum cleavage stress $\sigma_{\phi\phi}\max$ obtained from

$$\frac{\partial}{\partial o}\sigma_{oo}(r,o) = -\frac{3}{4}\frac{1}{\sqrt{2r}}\cos\frac{o^*}{2}\left[k_1\sin o^* + k_2(3\cos\phi^*-1)\right] = 0 \ ,$$

$$\sigma_{oo}(r,o^*) > 0 \tag{51a,b}$$

and at a value of the load level determined by

$$\sigma_{\theta\theta}(r,\sigma^*) = \frac{1}{\sqrt{2r}}\left(k_1\cos^2\frac{\theta^*}{2} - \frac{3}{2}k_2\sin\theta^*\right)\cos\frac{\theta^*}{2} = \frac{K_{IC}}{\sqrt{2\pi r}} \quad . \tag{52}$$

where K_{IC} is the (local) critical stress intensity factor of the medium. In studying the fracture initiation from an existing flaw in brittle and quasi-brittle nonhomogeneous materials, two additional points need to be made. The first concerns the angular distribution of the asymptotic stress state for small values of r. It appears that these expressions (such as (50)) for a nonhomogeneous medium are identical to that of a homogeneous medium provided near and at the crack tip the elastic properties of the medium are continuous (but not necessarily differentiable) functions of the space coordinates (see Delale and Erdogan, 1988a). The second point is that, even though the material is assumed to be isotropic with respect to its fracture resistance, the resistance parameter K_{IC} is expected to be a function of the space variables. K_{IC} may be determined from standard fracture toughness experiments by using a series of homogeneous specimens covering the complete range of material composition for the nonhomogeneous medium under consideration.

For a fixed value of $a\delta=1$ Table 3 shows the effect of loading conditions and the crack orientation on the normalized stress intensity factors. It may be observed that under certain individual loading conditions the mode I stress intensity factor k_1 could be negative, implying crack closure. Such solutions are, of course, not valid and can only be useful in a superposition that gives a positive resultant k_1.

In the solution given effect of the variation of the Poisson's ratio ν is assumed to be negligible. Analytically, it is difficult to verify this assumption. However, one can solve the problem for various different values of ν and compare the results. This is shown in Tables 4 and 5. Table 4 shows the effect of ν on the stress intensity factors for $a\delta=0.25$, $\theta=\pi/2$, and for uniform crack surface tractions $-\sigma_0$ and $-\tau_0$. The maximum difference observed was 2% in $\bar{k}_1$ under uniform crack surface pressure σ_0. The difference for other loading conditions (which are not all shown in the table) was somewhat smaller. For $\theta=0$ similar results were found by Delale and Erdogan, 1983. The effect of ν is, however, more significant for greater values of $a\delta$. For example, the same calculations as Table 4 were repeated for $a\delta=2.5$ and the results are shown in Table 5. It may be seen that the difference in $\bar{k}_1$ obtained from $0.05\leq\nu\leq0.45$ may be as high as 15%. On the other hand, within a more practical range of ν, namely for $0.2\leq\nu\leq0.35$, the difference is less than 6%.

Some additional results for displacement loading given by (45) are shown in Tables 6 and 7. The tables show the effect of the nonhomogeneity parameter $a\delta$ and the crack

orientation θ on the normalized stress intensity factors.

After solving the integral equations and observing that

$$\int_{-1}^{r} \frac{T_n(s)ds}{\sqrt{1-s^2}} = -\frac{1}{n} U_{n-1}(r)\sqrt{1-r^2} \quad . \tag{53}$$

the relative crack surface opening may easily be obtained from (22), (32), and (34) as follows:

$$u(x,+0)-u(x,-0) = \int_{-a}^{x} g_1(t)dt = -\sqrt{a^2-x^2} \sum_{1}^{\infty} \frac{1}{n} A_n U_{n-1}(x/a) \ ,$$

$$v(x,+0)-v(x,-0) = \int_{-a}^{x} g_2(t)dt = -\sqrt{a^2-x^2} \sum_{1}^{\infty} \frac{1}{n} B_n U_{n-1}(x/a) \quad . \tag{54a.b}$$

Figures 3 and 4 show the crack opening in y direction for δ=0.5 and 2.5, respectively, where the loading is crack surface pressure σ_o and the normalized displacements given in the figures are defined by

$$\bar{v} = \frac{1}{v_o} [v(x,0)-v(x,-0)] \quad , \quad v_o = \sigma_o \frac{1+\kappa}{2\mu_o} \quad . \tag{55}$$

The three displacements shown in each figure correspond to θ=0 and θ=π/2 with $\delta \neq 0$. and to a homogeneous material (δ=0). It may be seen that for large values of δ the crack opening displacements in nonhomogeneous materials can be significantly greater than the corresponding homogeneous values.

REFERENCES

Batakis, A.P. and Vogan, J.W., 1985, "Rocket Thrust Chamber Thermal Barrier Coatings", NASA CR-1750222.

Delale, F. and Erdogan, F., 1983, "The Crack Problem for a Nonhomogeneous Plane", ASME Journal of Applied Mechanics, Vol. 50, pp. 609-614.

Delale, F. and Erdogan, F., 1988a, "Interface Crack in a Nonhomogeneous Medium", Int. J. Engng. Sci., Vol. 26, pp. 559-568.

Delale, F. and Erdogan, F., 1988b, "On the Mechanical Modelling of the Interfacial Region in Bonded Materials", ASME Journal of Applied Mechanics, Vol. 55, pp. 317-324.

Dhaliwal, R.S. and Singh, B.M., 1978, "On the Theory of Elasticity of a Nonhomogeneous Medium", Journal of Elasticity, Vol. 8, pp. 211-219.

Erdogan, F., 1985, "The Crack Problem for Bonded Nonhomogeneous Materials Under Antiplane Shear Loading", ASME Journal of Applied Mechanics, Vol. 52, pp. 823-828.

Erdogan, F. and Sih, G.C., 1963, "On the Crack Extension in Plates Under Plane Loading and Transverse Shear", ASME Journal of Basic Engineering, Vol. 85, pp. 519-527.

Gerasoulis, A. and Srivastav, R.P., 1980, "A Griffith Crack Problem for a Nonhomogeneous Medium", Int. J. Engng. Sci., Vol. 18, pp. 239-247.

Hirano, T., Yamada, T., Teraki, J., Niino, M. and Kumakawa, A., 1988, "A Study on a Functionally Gradient Material Design System for a Thrust Chamber", Proc. 16th Int. Symposium on Space Technology and Science, Sapporo, Japan.

Hirano, T. and Yamada, T., 1988, "Multi-Paradigm Expert System Architecture Based Upon the Inverse Design Concept", Int. Workshop on Artificial Intelligence for Industrial Applications, Hitachi, Japan.

Houck, D.L., ed., 1987, Thermal Spray: Advances in Coatings Technology, Proc. of the National Thermal Spray Conference, Orlando, Florida, ASM International.

Kassir, M.K., 1972, "Note on the Twisting Deformation of a Nonhomogeneous Shaft Containing a Circular Crack", Int. J. Fracture Mechanics, Vol. 8, pp. 325-334.

APPENDIX

Expressions of the functions $K_{ij}(y,\alpha)$, $(i,j=1,2)$

$$K_{11}(y,\alpha) = e^{\gamma y}\left\{\frac{(3-\kappa)\alpha m_1+i(1+\kappa)n_1}{4\alpha(\kappa-1)\omega_0}[(1+\kappa)f_{32}-i\alpha(3-\kappa)f_{22}]e^{n_1 y}\right.$$

$$\left.+\frac{(3-\kappa)\alpha m_2+i(1+\kappa)n_2}{4\alpha(\kappa-1)\omega_0}[-(1+\kappa)f_{31}+i\alpha(3-\kappa)f_{21}]e^{n_2 y}\right\},$$

$$K_{12}(y,\alpha) = e^{\gamma y}\left\{\frac{(3-\kappa)\alpha m_1+i(1-\kappa)n_1}{4\alpha(\kappa-1)\omega_0}(1+\kappa)(f_{12}-i\alpha f_{42})e^{n_1 y}\right.$$

$$\left.-\frac{(3-\kappa)\alpha m_2+i(1-\kappa)n_2}{4\alpha(\kappa-1)\omega_0}(1-\kappa)(f_{11}-i\alpha f_{41})e^{n_2 y}\right\},$$

$$K_{21}(y,\alpha) = e^{\gamma y}\left\{\frac{\alpha+in_1 m_1}{4\alpha\omega_0}[(1-\kappa)f_{32}-i\alpha(3-\kappa)f_{22}]e^{n_1 y}\right.$$

$$\left.+\frac{\alpha+in_2 m_2}{4\alpha\omega_0}[-(1+\kappa)f_{31}+i\alpha(3-\kappa)f_{21}]e^{n_2 y}\right\},$$

$$K_{22}(y,\alpha) = e^{\gamma y}\left\{\frac{\alpha+in_1 m_1}{4\alpha\omega_0}(1-\kappa)(f_{12}-i\alpha f_{42})e^{n_1 y}\right.$$

$$\left.-\frac{\alpha+in_2 m_2}{4\alpha\omega_0}(1+\kappa)(f_{11}-i\alpha f_{41})e^{n_2 y}\right\},$$

$$\omega_0 = (m_1-m_2)(m_3-m_4)(n_1n_2+n_3n_4)+(m_1-m_4)(m_2-m_3)(n_2n_3+n_1n_4)$$

$$-(m_1-m_3)(m_2-m_4)(n_1n_3+n_2n_4)$$

where γ, m_i, n_i, and f_{jk} are given by (2), (11), (13), and (24), respectively.

Table 1. The effect of the nonhomogeneity constant β on the stress intensity factors; $\nu=0.3$, $p_1(x)=-\sigma_o$, $p_2(x)=0$, $\bar{k}_i(\mp a) = k_i(\mp a)/\sigma_o\sqrt{a}$.

a	0.1	0.25	0.5	1.0	2.5	5.0
$\beta = \pi/2$ ($\bar{k}_1(-a) = \bar{k}_1(a)$, $\bar{k}_2(-a) = -\bar{k}_2(a)$)						
$\bar{k}_1(a)$	1.008	1.036	1.101	1.258	1.808	2.869
$\bar{k}_2(a)$	0.026	0.065	0.129	0.263	0.697	1.567
$\beta = 0$ ($\bar{k}_2(a) = 0$, $\bar{k}_2(-a) = 0$)						
$\bar{k}_1(a)$	1.023	1.055	1.103	1.189	1.382	
$\bar{k}_1(-a)$	0.975	0.936	0.871	0.757	0.536	

Table 2. The effect of the nonhomogeneity constant ($a\delta$) and the crack orientation θ on the stress intensity factors; $\nu = 0.3$, $p_1(x) = -\sigma_0$, $p_2(x) = 0$, $\bar{k}_i(\mp a) = k_i(\mp a)/\sigma_0\sqrt{a}$

$a\delta$	θ/π	0	0.05	0.1	0.15	0.2	0.25	0.3	0.35	0.4	0.45	0.5
0.1	$\bar{k}_1(a)$	1.023	1.023	1.023	1.023	1.022	1.021	1.020	1.018	1.015	1.012	1.0085
	$\bar{k}_1(-a)$	0.975	0.976	0.977	0.980	0.983	0.987	0.991	0.996	1.0003	1.005	1.0085
	$\bar{k}_2(a)$	0.000	0.0052	0.0101	0.0146	0.0185	0.0217	0.024	0.026	0.027	0.027	0.0262
	$\bar{k}_2(-a)$	0.000	-0.0031	-0.0061	-0.0092	-0.0123	-0.0154	-0.018	-0.021	-0.023	-0.025	-0.0262
0.25	$\bar{k}_1(a)$	1.055	1.055	1.057	1.059	1.061	1.061	1.061	1.058	1.053	1.045	1.036
	$\bar{k}_1(-a)$	0.936	0.938	0.943	0.951	0.962	0.974	0.987	1.001	1.014	1.026	1.036
	$\bar{k}_2(a)$	0.000	0.016	0.030	0.043	0.054	0.061	0.067	0.069	0.070	0.068	0.065
	$\bar{k}_2(-a)$	0.000	-0.005	-0.011	-0.017	-0.024	-0.031	-0.039	-0.047	-0.054	-0.060	-0.065
0.5	$\bar{k}_1(a)$	1.103	1.106	1.113	1.123	1.133	1.141	1.145	1.143	1.135	1.120	1.101
	$\bar{k}_1(-a)$	0.871	0.875	0.887	0.906	0.931	0.960	0.990	1.021	1.050	1.077	1.101
	$\bar{k}_2(a)$	0.000	0.038	0.073	0.102	0.126	0.141	0.149	0.151	0.148	0.140	0.129
	$\bar{k}_2(-a)$	0.000	-0.006	-0.013	-0.022	-0.034	-0.048	-0.064	-0.082	-0.099	-0.115	-0.129
1.0	$\bar{k}_1(a)$	1.189	1.198	1.222	1.256	1.294	1.327	1.348	1.352	1.336	1.304	1.258
	$\bar{k}_1(-a)$	0.757	0.765	0.788	0.827	0.878	0.938	1.004	1.072	1.139	1.202	1.258
	$\bar{k}_2(a)$	0.000	0.093	0.179	0.251	0.306	0.339	0.352	0.346	0.327	0.298	0.263
	$\bar{k}_2(-a)$	0.000	-0.004	-0.010	-0.021	-0.039	-0.065	-0.099	-0.138	-0.181	-0.223	-0.263

Table 3. The effect of θ and the loading conditions on the stress intensity factors; ν = 0.3, a/b = 1.0, $\bar{k}_i(\mp a) = k_i(\mp a)/(\sigma_j, \tau_j)\sqrt{a}$.

θ/π	0	0.05	0.1	0.15	0.2	0.25	0.3	0.35	0.4	0.45	0.5
	$p_1(x) = -\sigma_1 x/a$, $p_2(x) = 0$										
$\bar{k}_1(a)$	0.479	0.479	0.480	0.483	0.487	0.494	0.503	0.514	0.525	0.534	0.540
$\bar{k}_1(-a)$	-0.486	-0.479	-0.493	-0.501	-0.511	-0.521	-0.530	-0.538	-0.542	-0.543	-0.540
$\bar{k}_2(a)$	0.000	-0.0032	-0.006	-0.006	-0.004	-0.0004	0.005	0.010	0.015	0.019	0.021
$\bar{k}_2(-a)$	0.000	0.0007	0.002	0.004	0.007	0.011	0.015	0.019	0.021	0.022	0.021
	$p_1(x) = -\sigma_2 x^2/a^2$, $p_2(x) = 0$										
$\bar{k}_1(a)$	0.545	0.547	0.553	0.562	0.571	0.579	0.584	0.585	0.582	0.575	0.565
$\bar{k}_1(-a)$	0.441	0.443	0.449	0.459	0.473	0.488	0.505	0.521	0.537	0.552	0.565
$\bar{k}_2(a)$	0.000	0.024	0.046	0.064	0.078	0.087	0.090	0.088	0.084	0.077	0.068
$\bar{k}_2(-a)$	0.000	-0.001	-0.003	-0.006	-0.012	-0.019	-0.027	-0.037	-0.048	-0.059	-0.068
	$p_1(x) = -\sigma_3 x^3/a^3$, $p_2(x) = 0$										
$\bar{k}_1(a)$	0.363	0.364	0.364	0.366	0.368	0.372	0.376	0.382	0.387	0.392	0.395
$\bar{k}_1(-a)$	-0.369	-0.370	-0.372	-0.376	-0.381	-0.386	-0.391	-0.394	-0.396	-0.397	-0.395
$\bar{k}_2(a)$	0	-0.001	-0.002	-0.003	-0.001	0.001	0.003	0.006	0.008	0.010	0.012
$\bar{k}_2(-a)$	0	0.0005	0.001	0.002	0.004	0.006	0.008	0.010	0.011	0.012	0.012
	$p_1(x) = 0$, $p_2(x) = -\tau_o$										
$\bar{k}_1(a)$	0.000	-0.003	-0.012	-0.030	-0.053	-0.082	-0.115	-0.149	-0.178	-0.198	-0.209
$\bar{k}_1(-a)$	0.000	0.038	0.076	0.111	0.141	0.166	0.184	0.198	0.207	0.211	0.209
$\bar{k}_2(a)$	1.189	1.187	1.179	1.169	1.154	1.136	1.116	1.094	1.069	1.038	0.999
$\bar{k}_2(-a)$	0.757	0.758	0.762	0.769	0.781	0.801	0.829	0.865	0.908	0.954	0.999

Table 3 - continued

θ/π	0	0.05	0.1	0.15	0.2	0.25	0.3	0.35	0.4	0.45	0.5
	$p_1(x) = 0,\ p_2(x) = -t_1 x/a$										
$\bar{k}_1(a)$	0.000	0.001	0.002	0.004	0.006	0.008	0.008	0.007	0.003	-0.003	-0.009
$\bar{k}_1(-a)$	0.000	-0.008	-0.016	-0.023	0.027	-0.029	-0.028	-0.025	-0.021	-0.016	-0.009
$\bar{k}_2(a)$	0.479	0.480	0.482	0.486	0.491	0.496	0.499	0.503	0.505	0.507	0.507
$\bar{k}_2(-a)$	-0.486	-0.486	-0.486	-0.487	-0.489	-0.492	-0.496	-0.500	-0.504	-0.506	-0.507
	$p_1(x) = 0,\ p_2(x) = -t_2 x^2/a^2$										
$\bar{k}_1(a)$	0.000	-0.002	-0.005	-0.010	-0.017	-0.024	-0.032	-0.041	-0.048	-0.052	-0.055
$\bar{k}_1(-a)$	0.000	0.011	0.021	0.031	0.039	0.045	0.050	0.053	0.055	0.056	0.055
$\bar{k}_2(a)$	0.545	0.544	0.542	0.540	0.536	0.531	0.527	0.522	0.516	0.509	0.500
$\bar{k}_2(-a)$	0.441	0.441	0.442	0.444	0.447	0.452	0.459	0.468	0.478	0.489	0.500
	$p_1(x) = 0,\ p_2(x) = -t_3 x^3/a^3$										
$\bar{k}_1(a)$	0	0.001	0.001	0.002	0.003	0.003	0.004	0.003	0.001	-0.002	-0.005
$\bar{k}_1(-a)$	0	-0.004	-0.009	-0.012	-0.014	-0.015	-0.015	-0.013	-0.011	-0.009	-0.005
$\bar{k}_2(a)$	0.363	0.364	0.365	0.368	0.370	0.372	0.374	0.376	0.378	0.379	0.379
$\bar{k}_2(-a)$	-0.369	-0.369	-0.369	-0.369	-0.370	-0.372	-0.374	-0.376	-0.377	-0.378	-0.379
	$\varepsilon_{y_1 y_1}(x_1, \mp a) = \varepsilon_o,\ \bar{k}_i(\mp a) = k_i(\mp a)/E_o \varepsilon_o \sqrt{a}$										
$\bar{k}_1(a)$	2.021	1.966	1.810	1.572	1.279	0.965	0.663	0.401	0.199	0.065	0
$\bar{k}_1(-a)$	0.442	0.435	0.413	0.377	0.325	0.258	0.182	0.103	0.035	-0.005	0
$\bar{k}_2(a)$	0	-0.210	-0.398	-0.541	-0.625	-0.642	-0.592	-0.485	-0.336	-0.166	0
$\bar{k}_2(-a)$	0	-0.072	-0.143	-0.208	-0.264	-0.305	-0.321	-0.303	-0.244	-0.141	0

Table 3 - continued

ℓ/a	0	0.05	0.1	0.15	0.2	0.25	0.3	0.35	0.4	0.45	0.5
	$\sigma_{y_1y_1}(x_1,\bar{+}\ell) = \sigma_1 x_1$, $\bar{k}_i(\bar{+}a) = k_i(\bar{+}a)/E_0\sigma_1\sqrt{a}$										
$\bar{k}_1(a)$	1.287	1.229	1.068	0.840	0.592	0.365	0.191	0.079	0.023	0.003	0
$\bar{k}_1(-a)$	-0.183	-0.179	-0.166	-0.146	-0.120	-0.090	-0.059	-0.031	-0.011	-0.002	0
$\bar{k}_2(a)$	0	-0.173	-0.310	-0.383	-0.385	-0.328	-0.236	-0.139	-0.061	-0.014	0
$\bar{k}_2(-a)$	0	0.028	0.053	0.073	0.085	0.087	0.078	0.059	0.034	0.011	0

Table 4. The effect of . on the stress intensity factors; a=0.25, =-/2, $\bar{k}_i(\bar{+}) = k_i(\bar{+}a)/(\tau_o,\tau_o)\sqrt{\bar{a}}$.

	0.05	0.1	0.15	0.2	0.25	0.3	0.35	0.4	0.45
	$p_1(x) = -\tau_o$, $p_2(x) = 0$, $(\bar{k}_1(-a) = \bar{k}_1(a), \bar{k}_2(-a) = -\bar{k}_2(a))$								
$\bar{k}_1(a)$	1.026	1.028	1.030	1.032	1.034	1.036	1.039	1.042	1.046
$\bar{k}_2(a)$	0.065	0.065	0.065	0.065	0.065	0.065	0.065	0.065	0.065
	$p_1(x) = 0$, $p_2(x) = -\tau_o$, $(\bar{k}_1(-a) = -\bar{k}_1(a), \bar{k}_2(-a) = \bar{k}_2(a))$								
$\bar{k}_1(a)$	-0.063	-0.063	-0.063	-0.063	-0.062	-0.062	-0.062	-0.062	-0.062
$\bar{k}_2(a)$	0.995	0.995	0.996	0.996	0.997	0.998	0.999	1.000	1.001

Table 5. The effect of and the loading conditions on the stress intensity factors; a = 2.5, = $\frac{-}{2}$, $\bar{k}_i(\bar{+}a) = k_i(\bar{+}a)/(\tau_j,\tau_j)\sqrt{\bar{a}}$.

	0.05	0.1	0.15	0.2	0.25	0.3	0.35	0.4	0.45
	$p_1(x) = -\tau_o$, $p_2(x) = 0$, $(\bar{k}_1(-a) = \bar{k}_1(a), \bar{k}_2(-a) = \bar{k}_2(a))$								
$\bar{k}_1(a)$	1.674	1.696	1.720	1.747	1.776	1.808	1.843	1.882	1.927
$\bar{k}_2(a)$	0.685	0.687	0.689	0.691	0.694	0.697	0.700	0.703	0.705
	$p_1(x) = -\tau_1 x/a$, $p_2(x) = 0$, $(\bar{k}_1(-a)=-\bar{k}_1(a), \bar{k}_2(-a)=\bar{k}_2(a)$								
$\bar{k}_1(a)$	0.633	0.638	0.643	0.649	0.656	0.663	0.671	0.680	0.690
$\bar{k}_2(a)$	0.082	0.083	0.084	0.085	0.086	0.087	0.088	0.090	0.091
	$p_1(x) = -\tau_2 x^2/a^2$, $p_2(x) = 0$, $(\bar{k}_1(-a)=\bar{k}_1(a), \bar{k}_2(-a)=-\bar{k}_2(a))$								
$\bar{k}_1(a)$	0.668	0.674	0.680	0.687	0.694	0.703	0.712	0.722	0.733
$\bar{k}_2(a)$	0.174	0.174	0.175	0.175	0.176	0.176	0.177	0.177	0.178
	$p_1(x) = 0$, $p_2(x) = -\tau_o$, $(\bar{k}_1(-a)=-\bar{k}_1(a), \bar{k}_2(-a)=\bar{k}_2(-a))$								
$\bar{k}_1(a)$	-0.405	-0.404	-0.402	-0.400	-0.399	-0.397	-0.395	-0.392	-0.390
$\bar{k}_2(a)$	0.989	0.996	1.003	1.011	1.019	1.028	1.038	1.048	1.060
	$p_1(x) = 0$, $p_2(x) = -\tau_1 x/a$, $(\bar{k}_1(-a)=\bar{k}_1(a), \bar{k}_2(-a)=-\bar{k}_2(a))$								
$\bar{k}_1(a)$	-0.020	-0.020	-0.020	-0.020	-0.021	-0.021	-0.021	-0.022	-0.022
$\bar{k}_2(a)$	0.527	0.528	0.529	0.531	0.532	0.533	0.535	0.537	0.539
	$p_1(x) = 0$, $p_2(x) = -\tau_2 x^2/a^2$, $(\bar{k}_1(-a)=-\bar{k}_1(a), \bar{k}_2(-a)=\bar{k}_2(a))$								
$\bar{k}_1(a)$	-0.106	-0.105	-0.105	-0.104	-0.104	-0.103	-0.103	-0.102	-0.102
$\bar{k}_2(a)$	0.499	0.501	0.503	0.505	0.508	0.510	0.513	0.516	0.519

Table 6. Normalized stress intensity factors for "uniform strain" $\varepsilon_{y_1y_1}(x_1, \mp\infty) = \varepsilon_o$ away from the crack region; $\nu = 0.3$, $K_o = E_o \varepsilon_o \sqrt{a}$.

a	c/a	$k_1(a)/K_o$	$k_1(-a)/K_o$	$k_2(a)/K_o$	$k_2(-a)/K_o$
0.25	0	1.196	0.825	0	0
	0.1	1.081	0.750	-0.321	-0.254
	0.2	0.781	0.548	-0.514	-0.422
	0.3	0.414	0.290	-0.504	-0.437
	0.4	0.121	0.075	-0.304	-0.282
	0.5	0	0	0	0
0.5	0	1.424	0.674	0	0
	0.1	1.285	0.617	-0.344	-0.213
	0.2	0.925	0.460	-0.548	-0.365
	0.3	0.490	0.247	-0.532	-0.397
	0.4	0.146	0.059	-0.314	-0.269
	0.5	0	0	0	0
2.5	0	6.317	0.115	0	0
	0.1	5.376	0.117	-0.867	-0.037
	0.2	3.315	0.115	-1.155	-0.090
	0.3	1.441	0.082	-0.900	-0.158
	0.4	0.369	0.004	-0.429	-0.179
	0.5	0	0	0	0

Table 7. Normalized stress intensity factors for "bending" away from the crack region; ν=0.3, $\varepsilon_{y_1y_1}(x_1,\pm\infty) = \varepsilon_1 x_1$, $K_1 = \varepsilon_1 E_o\sqrt{a}$.

a	x/a	$k_1(a)/K_1$	$k_1(-a)/K_1$	$k_2(a)/K_1$	$k_2(-a)/K_1$
0.25	0	0.637	-0.391	0	0
	0.1	0.542	-0.340	-0.174	0.111
	0.2	0.3[illegible]	-0.217	-0.232	0.158
	0.3	0.118	-0.088	-0.160	0.121
	0.4	0.016	-0.014	-0.049	0.042
	0.5	0	0	0	0
0.5	0	0.809	-0.304	0	0
	0.1	0.683	-0.268	-0.214	0.087
	0.2	0.397	-0.178	-0.278	0.128
	0.3	0.139	-0.076	-0.184	0.105
	0.4	0.018	-0.013	-0.053	0.039
	0.5	0	0	0	0
2.5	0	4.982	-0.039	0	0
	0.1	3.929	-0.039	-0.898	0.012
	0.2	1.880	-0.037	-0.968	0.024
	0.3	0.486	-0.028	-0.480	0.033
	0.4	0.043	-0.009	-0.094	0.023
	0.5	0	0	0	0

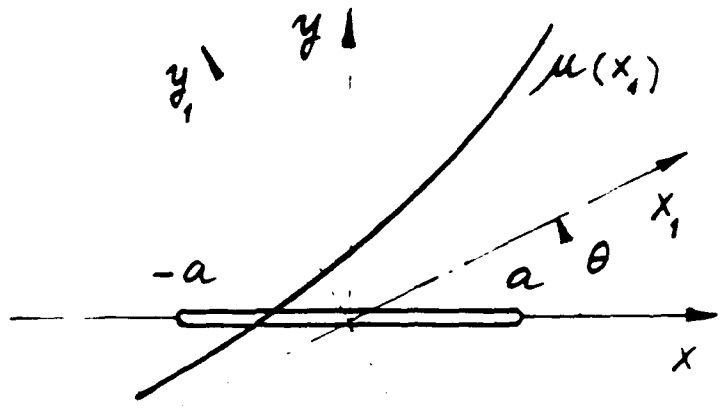

Fig. 1 Crack geometry in the nonhomogeneous medium

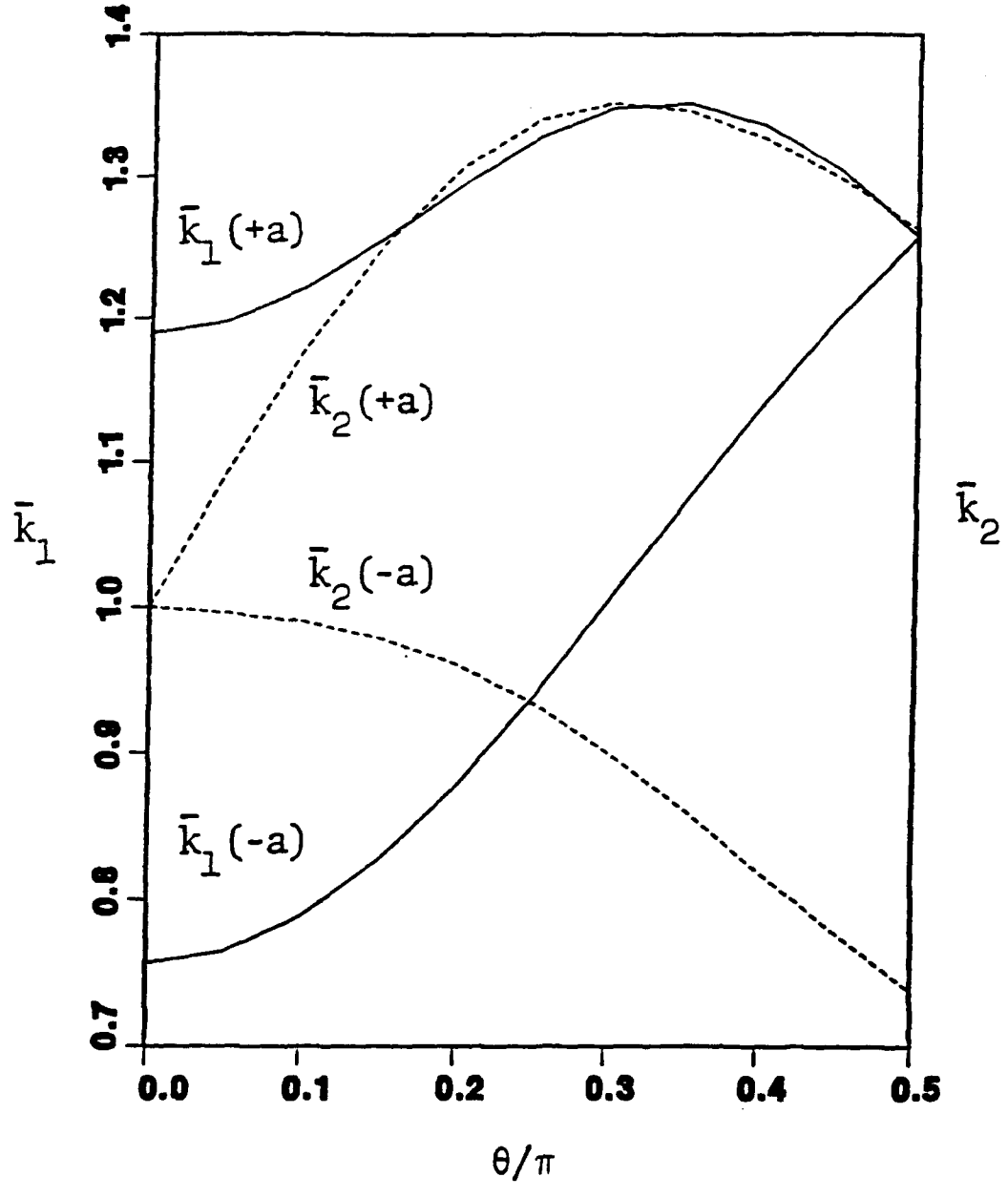

Fig. 2 Variation of the normalized stress intensity factors with the crack orientation in a nonhomogeneous medium containing a uniformly pressurized crack, $a\delta=1$.

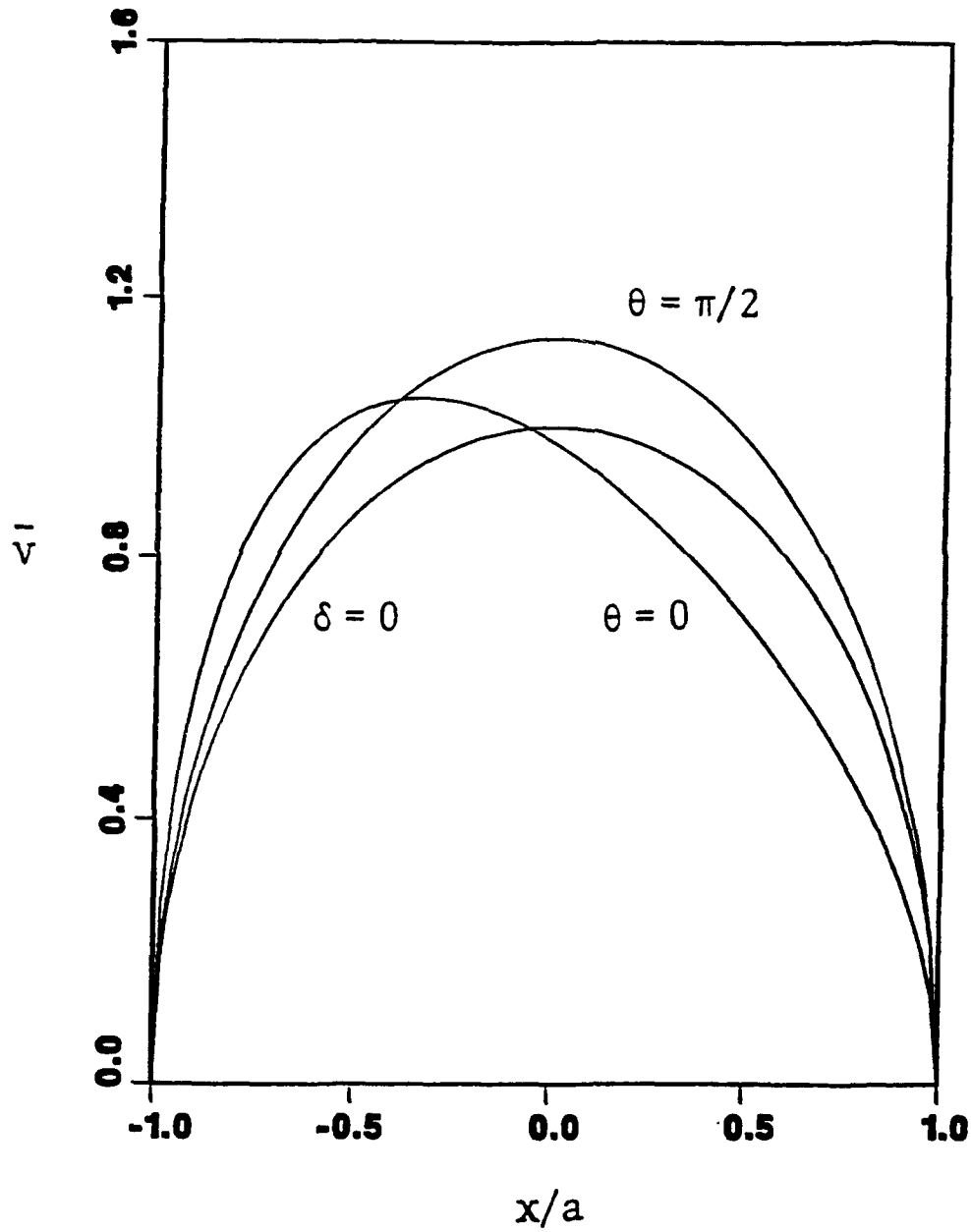

Fig. 3 Normalized relative crack opening in y direction for aδ=0.5, θ=0 and θ=-/2 and for a homogeneous medium (δ=0) (see Eq. 55).

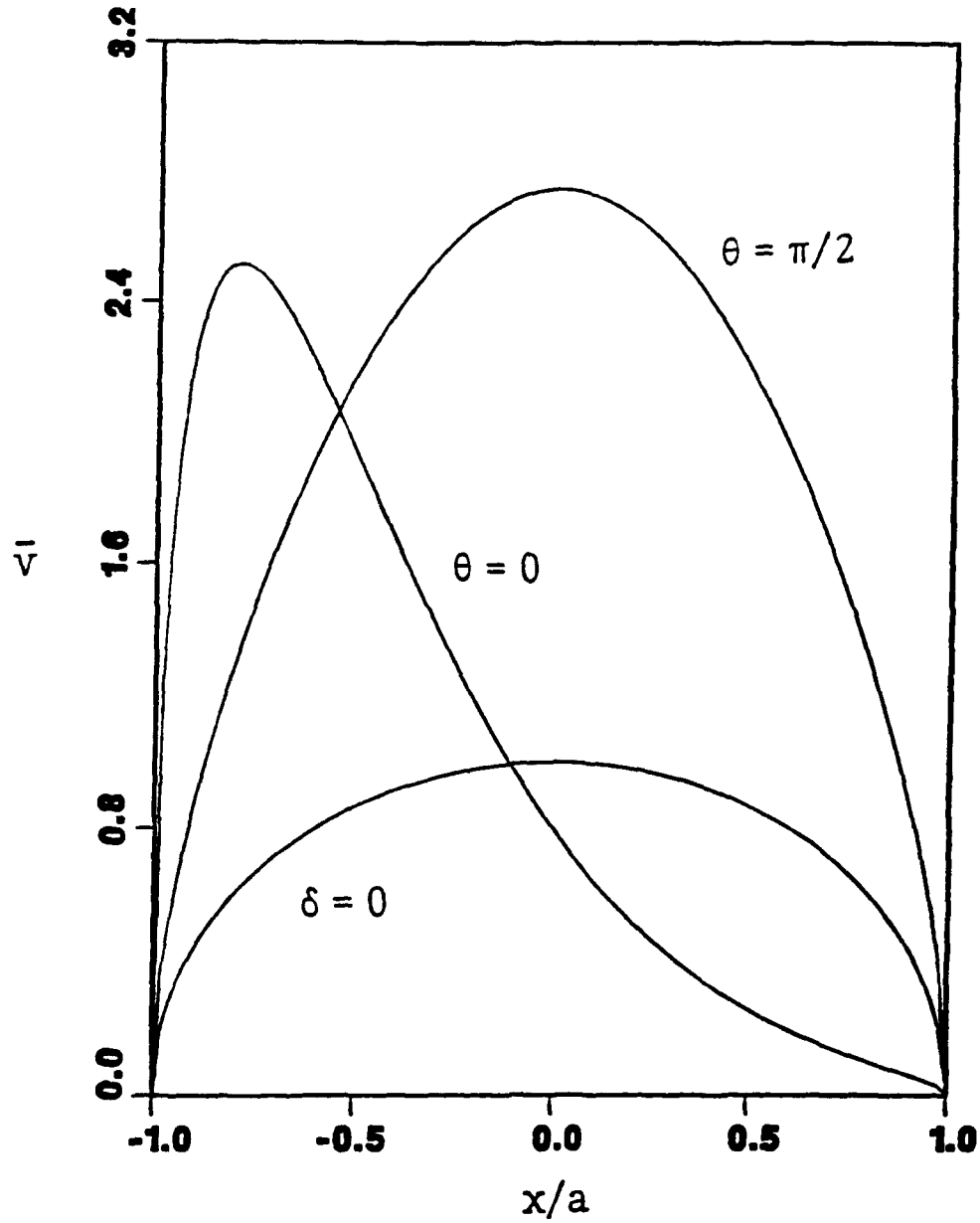

Fig. 4 Normalized relative crack opening in y direction for $a\delta=2.5$, $\theta=0$ and $\theta=\pi/2$ and for a homogeneous medium ($\delta=0$) (see Eq. 55).